Cancer Nanotechnology

RESEARCH Open Access

Early stage evaluation of cancer stem cells using platinum nanoparticles/CD_{133}^{+} enhanced nanobiocomposite

Solmaz Sadi[1], Balal Khalilzadeh[2*], Mahdi Mahdipour[2], Fatemeh Sokouti Nasimi[2], Ibrahim Isildak[3], Soodabeh Davaran[1], Mohammad-Reza Rashidi[4] and Farhad Bani[1*]

*Correspondence: khalilzadehb@tbzmed.ac.ir; balalkhalilzadeh@gmail.com; banif@tbzmed.ac.ir

[1] Department of Medical Nanotechnology, Faculty of Advanced Medical Sciences, Tabriz University of Medical Sciences, Tabriz 516661-4733, Iran
[2] Stem Cell Research Center, Tabriz University of Medical Sciences, Tabriz, Iran
[3] Department of Bioengineering, Faculty of Chemistry-Metallurgy, Yildiz Technical University, 34220 Istanbul, Turkey
[4] Department of Medicinal Chemistry, Faculty of Pharmacy, Tabriz University of Medical Sciences, Tabriz, Iran

Abstract

Background: Cancer stem cells (CSCs) are of great diagnostic importance due to their involvement in tumorigenesis, therapeutic resistance, metastasis and relapse.

Method: In this work, a sensitive electrochemical cytosensor was successfully established to detect HT-29 colorectal cancer stem cells based on a nanocomposite composed of mesoporous silica nanoparticles (MSNs) and platinum nanoparticles (PtNPs) using a simple and fast electrodeposition technique on a glassy carbon electrode (GCE).

Results: According to SEM images, the PtNPs nanoparticles formed on the MSNs substrate are about 100 nm. As expected, high-rate porosity, increased surface-to-volume ratio, provides appropriate local electron transfer rate and suitable platform for the efficient formation of PtNPs. These features allow direct and stable binding of biotinylated monoclonal antibody of CD_{133} to streptavidin (Strep) and the subsequent availability of active sites for CSCs identification. Differential pulse voltammetry (DPV) results show that close interaction of CD_{133}^{+} cells with monoclonal antibodies reduces charge transfer and electrical current, as confirmed by square wave voltammogram (SWV). Based on the recorded current versus number of CSCs, we noted that our developed system can sense CSCs from 5 to 20 cells/5 µL.

Conclusions: As a proof of concept, the designed nanobiocomposite was able to specifically detect CD_{133}^{+} cells compared to whole HT-29 cells before magnetic activated cell sorting (MACS) process.

Keywords: Cancer stem cells, CD_{133}, Platinum nanoparticles, Silica nanocomposite, Biosensor, Colorectal cancer

Introduction

Colorectal cancer, the second leading cause of cancer mortality, the second and third most common malignancies in men and women, respectively, is potentially treatable at stages 1 and 2 if early diagnosed (Ghoncheh et al. 2016). The 5-year survival in these stages is about 70–90% (Haggar and Boushey 2009). This index is reduced to 50–70%

and 10–14% in stages 3 and 4 cases, respectively (Ghoncheh et al. 2016). At stage 4, known as the distant (metastatic) era, the tumor branches out and spreads to distant organs and the lymph nodes through the blood and lymphatic vessels (Haggar and Boushey 2009; Markowitz and Bertagnolli 2009; Ricci-Vitiani et al. 2009). It is clear that early detection in the primary phases prevents metastasis and death. However, countries do not regularly implement colorectal cancer screening programs such as CT scans and MRI. In a tumor, in addition to the highly proliferating cells involved in the development of neoplasm mass and maintaining tumor growth, there is a small subset of undifferentiated slow cycle cells called cancer stem cells (CSCs) (Reya et al. 2001; Bomken et al. 2010). CSCs, as resemble tumor roots (Vinogradov and Wei 2012), exhibit the similar properties to self-regenerating embryonic stem cells (ESCs) such as unbounded proliferation and the potential for multidirectional differentiation (Melo et al. 2017; Bu and Cao 2012). The difference is that CSCs cause uncoordinated tumor growth due to their inability to inhibit excessive proliferation and differentiation (Ricci-Vitiani et al. 2009; Kreso and Dick 2014; Shimokawa et al. 2017). Common chemo and radiotherapy may reduce tumor volume and the number of somatic cancer cells from solid tumors, however, CSCs are generally not affected after these treatments (Hardin et al. 2017). These cells may escape treatment-induced damage by adopting resistance strategies, such as decrease of reactive oxygen species (Reya et al. 2001; Bomken et al. 2010; Diehn et al. 2009; Dalerba et al. 2007a; Baumann et al. 2008), increased DNA repair capacity, upregulation of metabolizing enzymes of cytostatic drugs such as aldehyde dehydrogenase (ALDH) and also expression of ABC transporters mediating multidrug-resistant (Kolodny et al. 2018; Pathania et al. 2018). After completing the treatment, hidden CSCs (Heddleston et al. 2010; LaBarge 2010) are potentially able to reconstruct a secondary tumor (Hosonuma et al. 2011; Tsai et al. 2011) and are supposed to be a means of metastasis to distant organs (Chiou et al. 2010; Croker et al. 2009). Brabletz and Oscarson groups considered two subgroups for colorectal CSCs: migratory cancer stem cells (MCSCs) and stationary cancer stem cells (SCSCs) (Brabletz et al. 2005; Oskarsson et al. 2014). Small fraction of circulating cancer stem cells (CCSCs) as agents for the development of new metastatic tumors, express CSC markers, including ALDH1, CD_{24}, CD_{44}, CD_{166} and CD_{133}(Dalerba et al. 2007a; Yang et al. 2015; Liao et al. 2014). CD_{133} is a membrane-bound pentaspan glycoprotein which is involved autophagy, matrix metalloproteinase functions and resistance to photodynamic therapy (PDT) and other variety of cellular processes (Li et al. 2012; Chenaghlou et al. 2021). Recent studies have indicated that therapeutic practices, including chemotherapy and radiation in CD_{133}^{+} stem like cells, can increase the autophagic response in these cells (Dalerba et al. 2007b; Kazama et al. 2018; Chen et al. 2010; Todaro et al. 2010). As a result of a study, unlike CD_{133}^{-} cells, the isolation of CD_{133}^{+} cells from colorectal tumors and then injection into mice led to niching and reconstructing tumors (Ricci-Vitiani et al. 2007; O'Brien et al. 2007). To this end, accurate detection of rare and heterogeneous numbers of MCSCs in body fluids: urine, blood and saliva require the design and construction of highly sensitive platforms (Ozkumur et al. 2013; Fachin et al. 2017). Despite several advantages in common cancer diagnosis techniques including flow cytometry, polymerase chain reaction (PCR) and immunohistochemistry, they are relatively expensive, need experts, time-consuming, and also have low sensitivity (Xu et al. 2020). Recently, many efforts

have been made to build portable electrochemical cell measurement tools by using low cost and biocompatible nanomaterials to identify the type, number and physiological parameters of the cells with selectivity and satisfactory sensitivity, easy operation and low or non-invasion and rapid response (Hasanzadeh et al. 2009; Nasrollahpour et al. 2021a; Rasouliyan et al. 2021; Saghatforoush et al. 2009; Same et al. 2022; Vandghanooni et al. 2021; Babaei et al. 2010). In this work, a nanobiocomposite of mesoporous silica and platinum nanoparticles conjugated with CD_{133} monoclonal antibody designed for cytosensing of HT-29 CSCs-CD_{133}^{+}. Mesoporous silica nanostructure which applied as a substrate for effective foundation of PtNPs, due to its interest porosity, increases the mass and charge transfer of electroactive species thus improves electrical conductivity. The PtNPs along with conductivity, enhance the direct and stable binding of biotinylated antibodies via streptavidin immobilization. The organic–inorganic chemical composition of tetraethyl orthosilicate ($Si(OEt)_4$) with desirable properties like mechanical strength, chemical and thermal stability, simple preparation via applying a negative potential under acidic conditions, provides a biocompatible platform in the construction of electrochemical based biosensors (Ciriminna et al. 2013; Farghaly and Collinson 2016; Isildak et al. 2020; Karimzadeh et al. 2020; Mansouri et al. 2020; Nasrollahpour et al. 2021b, 2021c). The electrodeposition method established both MSNs/PtNPs substrate at the same time in an environmentally friendly manner known as the green synthesis. This process makes nanocomposites preparation done in one- pot, fast and especially low cost. Some properties of nanocomposites such as thickness and porosity can be adjusted by modifying the parameters of the manufacturing process like deposition time, potential and concentration (Farghaly and Collinson 2014; Rezapour Sarabi et al. 2022). Applying a negative potential at the optimal time, following OH- hydrolysis of ethanol and water and condensing TEOS monomer precursors on the working electrode, creates a mesoporous silica film (Deepa et al. 2003; Sibottier et al. 2006; Goux et al. 2009). Metal nanoparticles electrogeneration in basic conditions and direct reduction of metal ion complexes are among the methods that provide the electrodeposition of PtNPs from solution to the electrode surface (Therese and Kamath 2000).

Experimental

Materials

Tetraethyl orthosilicate (TEOS), chloroplatinic acid hexahydrate ($H_2Cl_6Pt.6H_2O$), 6-mercapto-1-hexanol (MCH), hydrochloric acid and streptavidin were obtained from Sigma. Biotinylated monoclonal antibody of CD_{133} protein was purchased from Novus Biologicals. Streptavidin-coated magnetic beads (MyOne) was purchased from Invitrogen. Merck products H_2SO_4, Na_2HPO_4, KH_2PO_4, $NaNO_3$, KCl, HNO_3, NaOH, Al_2O_3 and NaCl were used. Absolute ethanol and paraformaldehyde (PFA) were obtained from Scharlau and Fluka, respectively. Finally, the solutions purchased from Gibco include Trypsin–EDTA, penicillin/streptomycin (P/S), TrypLE and DMEM/LG.

Apparatus

Metrohm Autolab equipped with Nova software provided electrochemical synthesis and exploring of electrical signal changes on glassy carbon electrodes. The operation on the working, counter, and reference electrodes was organized by actuators of glassy

carbon (2 mm diameter), Platinum wire and silver/silver chloride (Ag/AgCl) electrodes, respectively. The acidity/basicity of the prepared material was measured using a pH meter (Corning, 120) also a magnetic stirrer (Heidolph) and an ultrasonic device (Transonic 420) were employed for homogenization. SEM imaging of electrodeposited nanocomposite was done by TESCAN MIRA3 instrument.

In situ synthesis of MSNs/PtNPs

Co-electrodeposition of MSNs/PtNPs nanocomposite was regulated according to the process described in the article (Xu et al. 2020). Briefly, a solution consisting of 100 µL TEOS monomer, 5 mL ethanol (C_2H_5OH), 4 mL double-distillated H_2O (water) and 0.16998 g $NaNO_3$ (sodium nitrate) was prepared. After aging for 1 h in 350 rpm, the sol–gel solution was obtained. The solution was prepared by adding 1 mL of 0.63 mM platinum salt ($H_2Cl_6Pt.6H_2O$) and 300 µL of HCl (0.1 mM) Finally, it was transferred to an electrochemical cell for electrodeposition at the optimal potential and time using chronoamperometry technique ($E=-1.23$ V for 50 s). The obtained electrode was nominated as PtNPs/MSNs-GCE.

Immobilization of streptavidin on MSNs/PtNPs modified electrode

At this stage, an appropriate amount of streptavidin was incubated at specific time on the electrode. To do this, 5 µL of 25 µg/mL streptavidin was coated at 4 °C for 3 h then to remove unattached material the Strep-PtNPs/MSNs-GCE was soaked in PBS for five minutes. Electrochemical techniques were applied to investigate the electrochemical behavior in a solution containing 0.1 M KCl, 5 mM potassium ferrocyanide and potassium ferricyanide in a ratio of (1:1). Ascending potentials were scanned from −0.6 to 0.2 V at 0.1 V/s.

Immobilization of monoclonal antibody of CD_{133} on the modified electrode

Here, 5 µL of 0.6 µg/mL biotinylated anti-CD_{133} was dropped on modified electrode (Strep-PtNPs/MSNs-GCE) and incubated for 2 h at 4 °C and after immersing in PBS, its electrical current changes were recorded according to the previous procedure. The obtained electrode was nominated as Ab-Strep-PtNPs/MSNs-GCE.

Cell culture

HT-29 cell line, bought from the Pasteur Institute of IRAN, and cultured in low glucose (DMEM) supplemented with 7% fetal bovine serum (FBS) and 1% P/S, at 5% CO_2 in a 37 °C humid incubator. Following growth and achieving 80% of confluency, the cells were detached from culture flasks, adding TrypLE, collected and centrifuged in 1500 rpm at 10 min, then washed. Cell count was revealed using a Neubauer hemocytometer chamber.

Magnetic activated cell sorting (MACS)

In the following the biotinylated CD_{133} antibody were incubated with streptavidin-coated magnetic beads (MyOne), mixed every 15 min for 5 h. Then the HT-29 cells suspension mixed with CD_{133} antibody-beads for 2 h at 4 °C. After washing the MACS column, the incubated cells with CD_{133}-MyOne beads were passed through a LS-column. Finally, the

cells crossed the column as negative control and the remaining cells in the column were separated from the column and used as CD_{133}^{+} cells and subjected to the calibration curve. It should be noted that, negative and positive cells were counted and about 1.75% of the cells was noted to be CD_{133}^{+}.

Results

Investigation of electrodeposition of MSNs/PtNPs on the working electrode

To achieve the optimal potential of the desirable co-electrodeposition of MSNs/PtNPs nanocomposite on the GCE, the solution content monomers of nanocomposite deposited in constant time (40 s) and different potential via CHA technique (−1.1 to −1.25 V) and signal amplification were checked through DPV technique. Finally, the best nanocomposite for signal amplification was observed at (E = −1.23 V for 50 s).

Effect of MSNs/PtNPs

To investigate the synergistic signal amplification of nanocomposite, MSNs and PtNPs were synthesized individually. The peak heights obtained from both were compared with the total current. Their peak height was less than the co-electrodeposition of the nanocomposite. The comparison of peak currents is illustrated in Fig. 1.

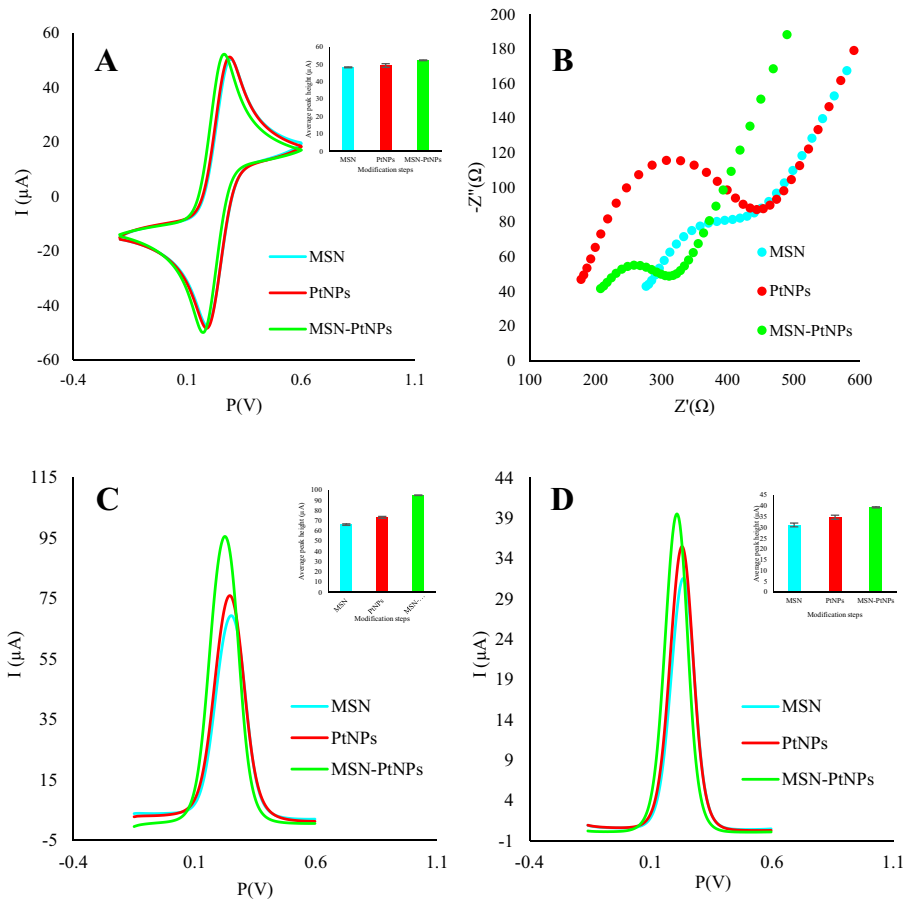

Fig. 1 Signal amplification in co-electrodeposition of MSNs/PtNPs nanocomposite in CV (**A**), EIS (**B**), SWV (**C**) and DPV (**D**) techniques with their histograms

PtNPs was probably deposited as an incomplete film with low density so the signal amplification was weaker than when electrosynthesized simultaneously with MSNs. The porosity formed in mesoporous silica increases the surface-to-volume ratio, improves the electron transfer rate and provides a suitable place for the genesis of active platinum nanoparticles.

Optimization of the incubation time of streptavidin

After attaining the appropriate concentration of streptavidin at 4 °C, the optimal incubation time at the proper concentration was checked. To do that, 5 µL of 25 µg/mL streptavidin was coated on PtNPs/MSNs-GCE for various times of (2, 3, 6 and 24 h). According to the recorded DPV histogram, 3 h incubation seems to be the most appropriate time for streptavidin layering in PtNPs/MSNs-GCE, whereas overcoating of the modified electrode in excess time led to electrical insulation. The incubation time of streptavidin is shown in Fig. 2.

Optimization of monoclonal biotinylated CD_{133} antibody concentration

To obtain the suitable concentration of the monoclonal antibody on the modified electrode, four different concentrations of Ab-CD_{133} (60, 6, 0.6, 0.006 µg/mL) were

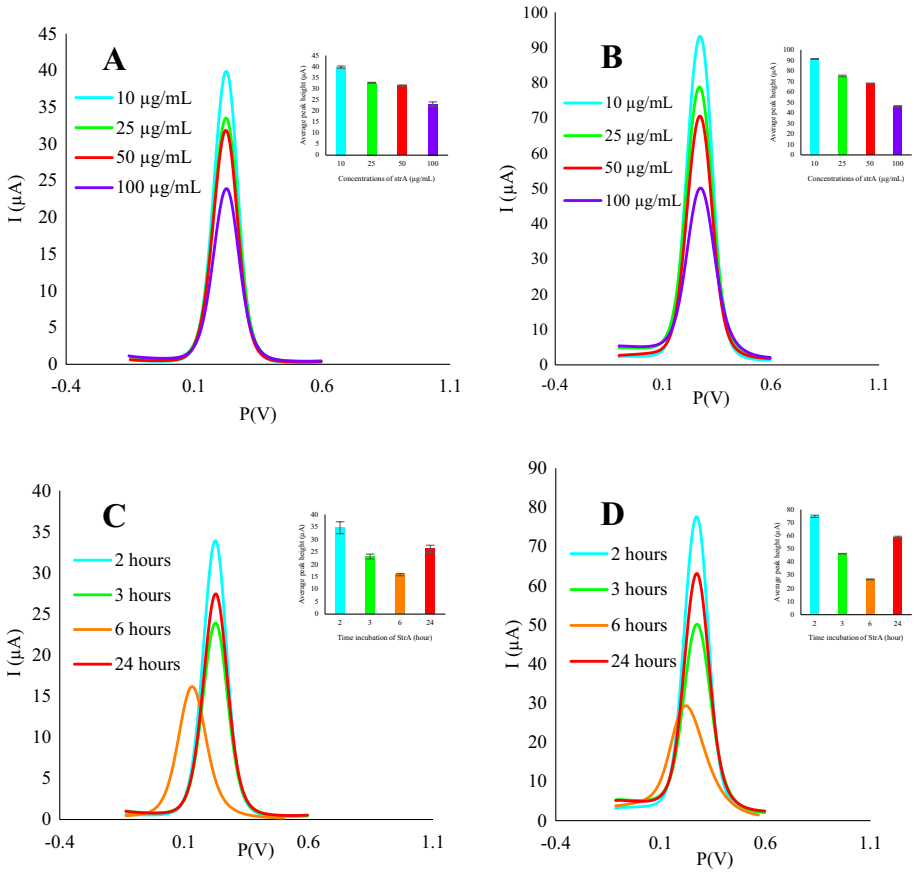

Fig. 2 Optimization of concentration of streptavidin **A** DPV, **B** SWV and their histograms. Optimization of incubation time of streptavidin, **C** DPV and **D** SWV and their histograms

immobilized on Ab-Strep-PtNPs/MSNs-GCE and incubated for 2 h at 4 °C. At a concentration of 0.6 µg/mL, not only the DPV peak height reduction is not notable, but also can cover the electrode surface optimally and create high efficiency active sites. Therefore, it was a favorable antibody concentration for next step.

Optimization of the incubation time of monoclonal antibody of CD_{133}

After reaching the appropriate concentration of anti-CD_{133} and incubation temperature, the optimal incubation time was investigated. To do this, 5 µL of 0.6 µg/mL anti-CD_{133} was coated on modified GCE at various times (0.5, 1, 2, 3 and 4 h) and then, as in the previous steps, the peak height was monitored by DPV and SWV techniques. The results showed that 2-h period was sufficient time for stable incubation and direct binding via biotin–streptavidin antibody while maintaining the efficiency. The optimization of incubation time of the capture antibody is presented in Fig. 3.

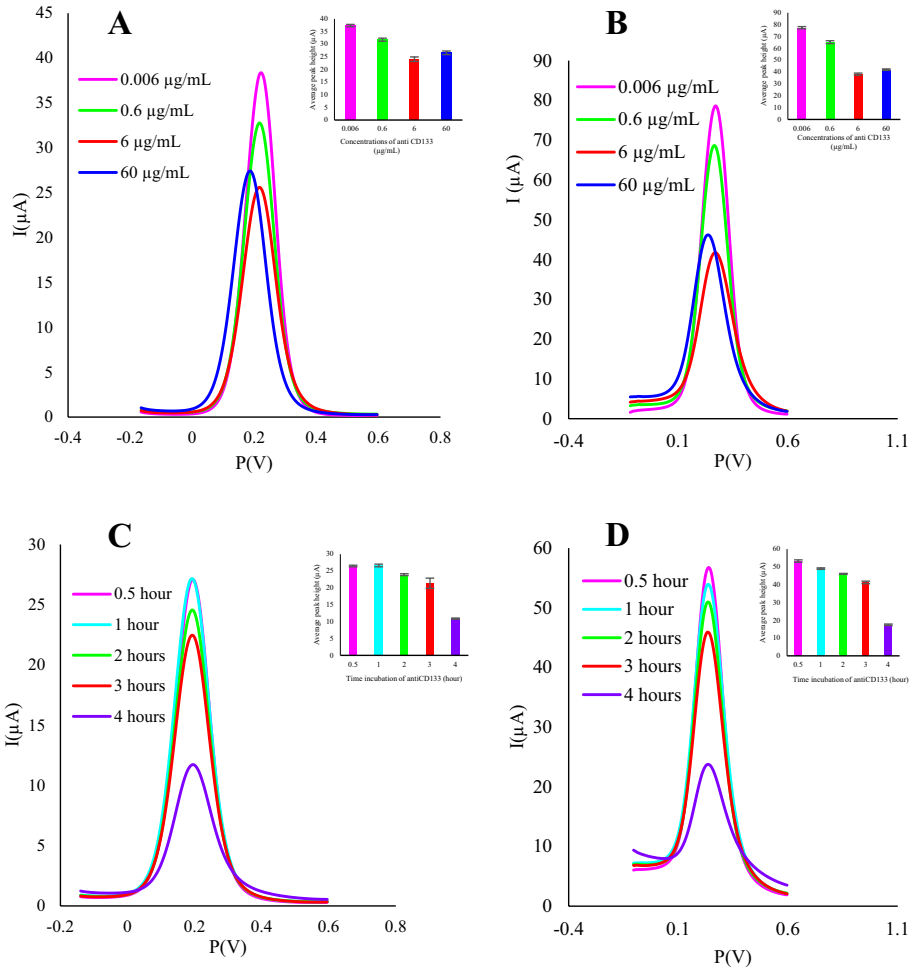

Fig. 3 Optimization of concentration of anti-CD_{133} **A** DPV, **B** SWV and their histograms. Optimization of incubation time of anti-CD_{133}, **C** DPV and **D** SWV and their histograms

Electrode preparation steps

The glassy carbon electrode was first washed physically and electrochemically by polishing alumina and then applying potentials in a solution of sulfuric acid and sodium hydroxide, respectively. Then PtNPs/MSNs nanocomposite was electrodeposited by applying the optimum potential at the optimum time (−1.23 V for 50 s). Subsequently, the 25 µg/mL of streptavidin was incubated on the PtNPs/MSNs/GCE for 3 h at 4 °C. Finally, the 0.6 µg/mL of biotin-containing anti-CD_{133} was stabilized on Strep-PtNPs/MSNs-GCE for 2 h at 4 °C. Eventually 5 µL of 1 µM MCH was poured onto the electrode for 30 min to block unspecified sites. At the end the electrode was washed carefully with PBS. The electrode preparation steps were step by step confirmed via different electrochemical techniques and presented in Fig. 4.

Study of surface morphology and properties

The surface of the fabricated cytosensor at each stage of the foundation was examined morphologically. Figure 5 shows clear scanning electron microscopy (SEM) images of the porous structure formed on the electrode and the proper stabilization of cancer stem cells on a modified electrode at different magnifications. In order to validate the correct operation processes dot mapping and energy dispersive X-ray

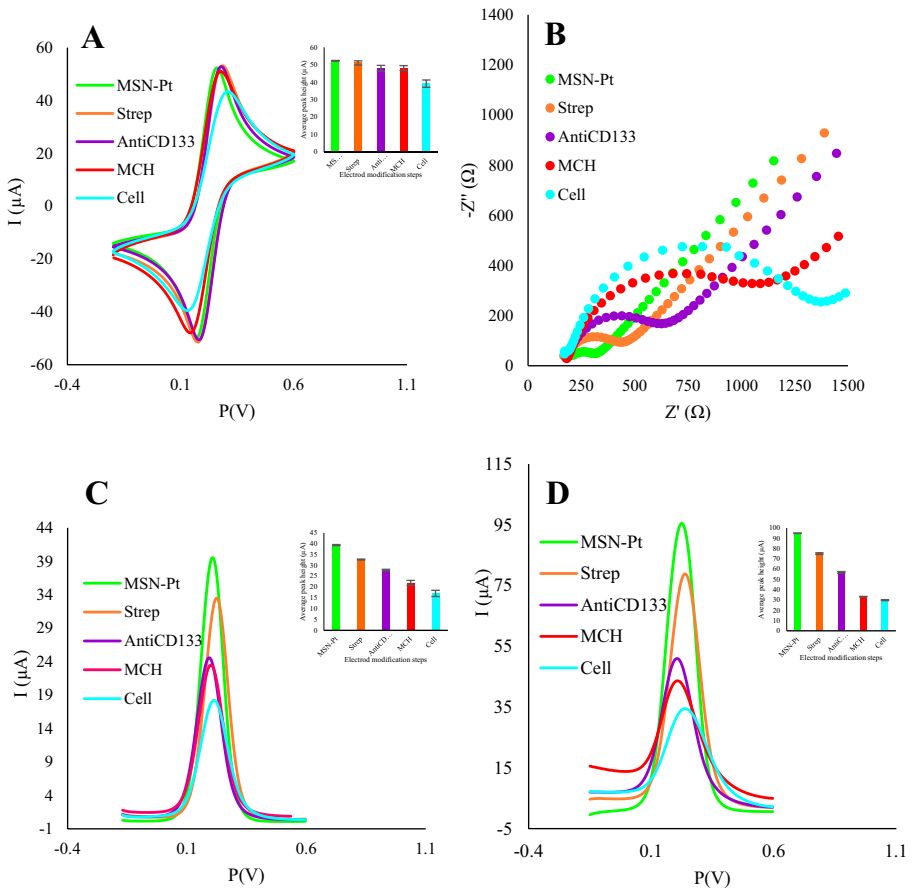

Fig. 4 Electrode preparation steps in different electrochemical techniques **A** CV, **B** EIS, **C** DPV, **D** SWV

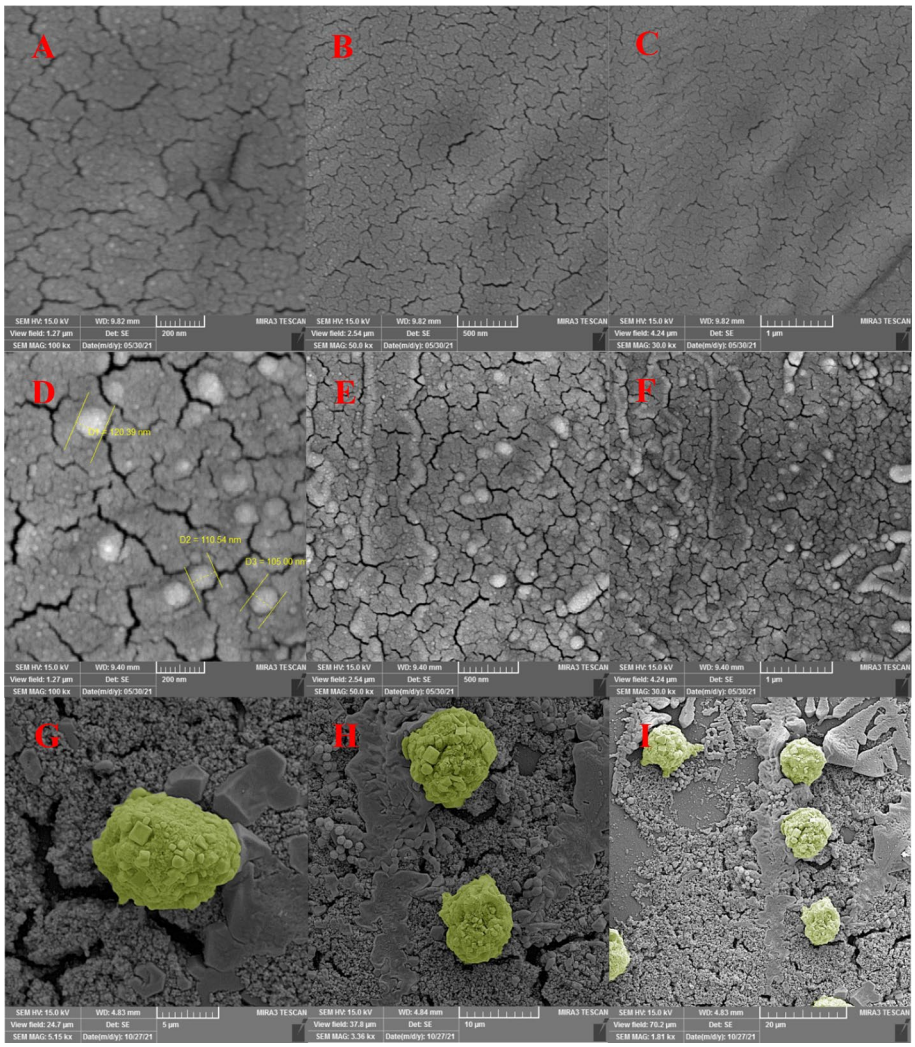

Fig. 5 **A**–**C** SEM images of the electrodeposited MSNs on the GCE, **D**–**F** co-electrodeposition of MSNs/PtNPs nanocomposite, and **G**–**I** immobilized cells on the modified electrode (CD_{133}^{+} cells-Ab-Strep-PtNPs/MSNs-GCE) in different magnifications

(EDX) were checked. The presence of silica, oxygen and platinum atoms shown in Additional file 1: Table S1 confirms the successful formation of PtNPs/MSNs on the GCE.

Calibration curve

To expose the analyte and plot the calibration curve, a certain number of picked up CD_{133}^{+} cells were incubated on the modified electrode (CD_{133}^{+} cells-Ab-Strep-PtNPs/MSNs-GCE) at 37 °C for 1 h, and then rinsed in PBS slowly. The linear range of 5–20 cells in SWV technique demonstrated CD_{133}^{+} CSCs was detected by the proposed cytosensor with $R^2 = 0.9642$. The calibration curve and related voltammograms are shown in Fig. 6.

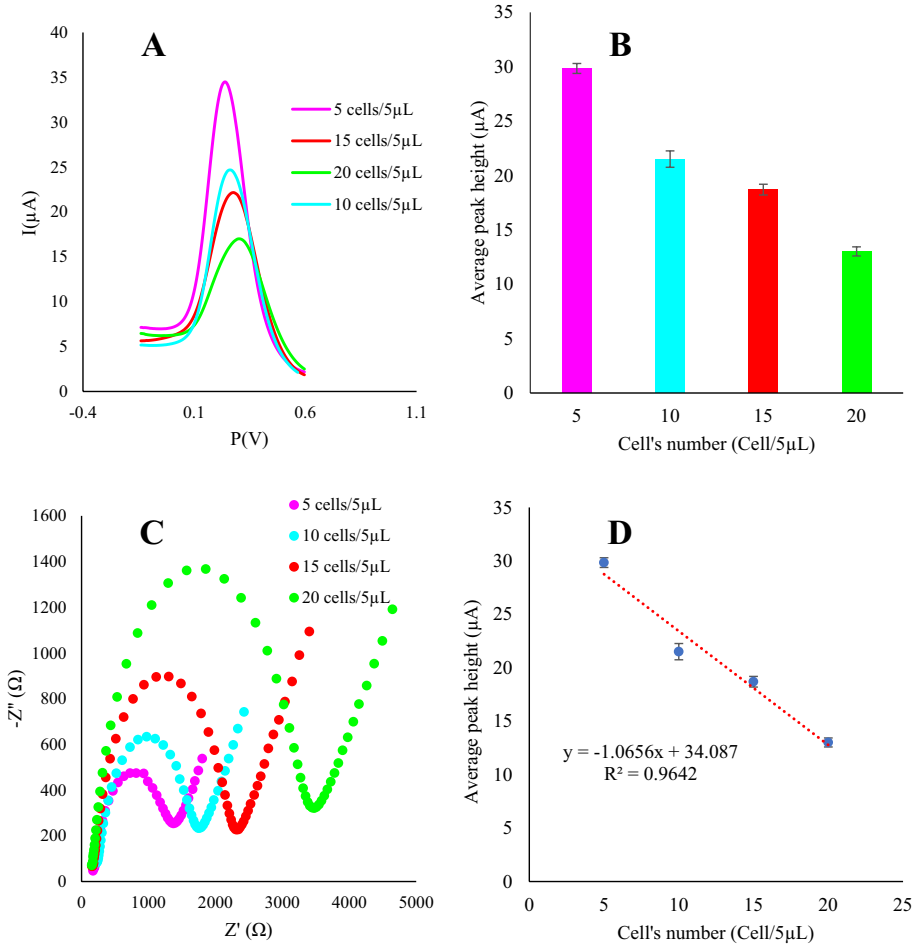

Fig. 6 Calibration curve, **A** the SWV technique's response in different number of CD_{133}^+ cells, **B** the SWV technique's histogram, **C** the EIS technique's response in different number of CD_{133}^+ cells, and **D** the linear relationship between the peak heights versus the cells number

Repeatability, reproducibility, stability and selectivity

To evaluate the cytosensor repeatability, the RSD calculation obtained from the SWV voltammogram for a concentration of 5 cells in 5 µL of CD_{133}^+ HT-29 for five repetitive measurements was about 1.5%. This satisfactory repeatability refers to the unique and regular synthesis of MSN-PtNPs in GCE as well as the direct binding of antibodies via the streptavidin to the nanocomposite.

The analytical performance of the two processed GC electrodes at the concentration of 20 cells/5 µL HT-29 CSC was evaluated in the same way. The attained relative standard deviation (RSD) of 1.35% indicates satisfactory cytosensor reproducibility. To check the stability of the cytosensor, 8 repetitions were recorded from SWV voltammograms. It should be noted that the SWV voltammetry technique was repeated by scanning the potential from −0.6 to 0.2 V at scan rate of 0.1 V/s in an electrochemical cell. The RSD of the obtained results was 2.66% at the concentrations of 15 cells/5 µL, indicating its suitable stability. In the selectivity test, following incubation of somatic cancer cells (SCC) and cancer stem cells (CSC) under the same experimental conditions, comparing DPV responses verified the selective diagnosis of CSC by the proposed cytosensor.

As shown in Additional file 1: Fig. S3, the selectivity experiments were performed on three different concentrations 5, 15 and 20 cells/5 μL. Remarkable decrease was not observed in electrochemical signals resulting from the somatic cancer cells, which could be indicate that the expression of CD_{133} on the CSC surface is significant (roughly two times) in comparison with the somatic cancer cells.

The comparative results showed the good selectivity of the developed cytosensor.

Discussion

Various nano-electrochemical cytosensors have been explored, with the aim of building a device for accurate, highly sensitive and specific sensing, using a variety of nanomaterials in various synthesis methods for evaluation of cancer cells which was studied summarized in **f**. A sandwich-type electrochemical cytosensor has been designed based a two-step binding recognition mechanism of tumor necrosis factor-related apoptosis-inducing ligand (TRAIL) on leukemia cells surface to HRP-TRAIL-Fe_3O_4@Au hybrid nanoprobes and the quantitative characterization of DR4/DR5 expression status on cell surfaces through dendrimer-stabilized Au nanoparticles (Au DSNPs) (Zheng et al. 2013). It was noted that the sandwich-type cytosensor improves CTCs capture efficiency and boosts the sensitivity by reason of the binding and detection of surface proteins on both cell sides, however, designing and fabrication of probes is quite complex and multi-stage, time-consuming and costly. Besides, prolonged antibody incubation, reducing the amount of proper binding resulting from random and non-specific binding, are some of the challenges that need to be addressed. Apart from the challenges on the complexity and prolongation of nanostructures and nanoprobes processing time in sandwich-type electrochemical sensors, the issue of environmental and personal damage in dealing with harmful substances in this type of procedure is worth considering. Likewise, the stability and adhesion of chemically processed nanostructures on the electrode is reduced because they are spread on the electrode. Naturally, the distribution and dripping of them on the electrode has little stability and adhesion. Maintaining the stability and efficiency of HRP-labeled metal nanoprobes prepared during a long process and consuming high thermal energy is another problem of the biosensor durability. Overall, the response time of the bioassay increases following the long incubation time of the nanoprobes in sandwich strategy (Sun et al. 2016). In this work, a novel PtNPs/MSNs nanocomposite was designed for a label-free, rapid and sensitive cytosensing of HT-29 CSCs. Both materials of this biocompatible nanocomposite were simultaneously co-electrodeposited in less than one minute. Electrodeposition method applied is a simple approach for in situ, fast and one pot composing of PtNPs/MSNs nanocomposite. It is also a type of green synthesis which minimizes the consumption and production of pollutants and environmentally harmful waste (The summary of the previously prepared cytosensors for the evaluation of CTCs is shown in Table 1).

Conclusion

Evaluation of CSCs-CD_{133}^{+} based on PtNPs/MSNs nanocomposite in the electrochemical platform succeeded in tracking linear range of 5–20 cells/5 μL suitable for cancer detection in the early stages of tumor formation. It has a significant sensitivity compared to flow cytometry as a reference method. So may be a good candidate for use in integrated diagnostic tools for low-cost clinical diagnosis if other antibodies specific to this

Table 1 A summary of the proposed cytosensors for the evaluation of CTCs

Working electrode	Platform	System	Cell type	DL (cells mL^{-1})	LDR (cells mL^{-1})	Refs.
GCE[1]	HRP[2]-TRAIL[3]-Fe_3O_4@Au Au DSNPs[4]/PDCNx	CV	HL-60 & Jurkat		40	Zheng et al. (2013)
GCE	AuNPs[6]/pTTBA[7]/CapAnti[8](nCOL)[9]-AuNPs-(Hyd)[10]	EIS	SK-BR3 & MCF-7	28	45–100,000	Pallela et al. (2016)
GCE	G-3D[11]-Au	EIS & CV	143B	1292	5.0×10^3 to 5×10^6	Wu et al. (2018)
MGCE[12]	(rGO[13]/MoS_2[14])-Fe_3O_4NPs	EIS & CV	MCF-7	6	15 to 45	Tian et al. (2018a)
GCE	Fe_3O_4/MnO_2/Au@Pd–HRP–probe MCH[15]/aptamer/AuNPs	EIS & DPV	HepG2	15	1×10^2 to 1×10^7	Sun et al. (2016)
GCE	CNS[16]@AuNP/chitosan	DPV	A549	14	4.2×10^{-1} to 4.2×10^{-6}	Zhang et al. (2019)
PWE[17]	Au@3D-rGO/PH–Au@Pd NPs[18]	DPV & colorimetric	MCF-7	20	50 to 10^7	Wang et al. (2018)
GCE	rGO/AuNPs-CuO	DPV	MCF-7	27	50 to 7×10^3	Tian et al. (2018b)
NC[19]	AuNPs–SSEA-4 antibody conjugates	Naked eye or strip reader	hPSCs[21]	10,000	1×10^4 to 2×10^5	Wu et al. (2013)
GCE	MSN[20]-Pt	DPV and SWV	CSC	5	5 to 20	This work

1. glassy carbon electrode, 2. horseradish peroxidase, 3. tumor necrosis factor (TNF) related apoptosis-inducing ligand, 4. dendrimer-stabilized Au nanoparticles, 5. poly(diallyl dimethylammonium chloride) nitrogen-doped carbon nanotubes, 6. gold nanoparticles, 7. 5.2,2′:5′,2″-terthiophene-3′ p-benzoic acid, 8. capture antibody, 9. nanostructured collagens, 10. hydrazine, 11. graphene-three-dimensional nanostructure gold nanocomposites, 12. magnetic glassy carbon electrode, 13. reduced graphene oxide, 14. molybdenum disulfide, 15. 6-mercapto-1-hexanol, 16. monodisperse colloidal carbon nanospheres, 17. paper working electrode, 18. polyhedral-Au@Pd alloy nanoparticles, 19. nitrocellulose membranes, 20. mesoporous silica nanostructure, 21. human pluripotent stem cells

cell line are involved. The fusion of the mesoporous structure of silica beside active and adhesive PtNPs, increases the mass and charge transfer rate, and provide many active sites for the binding of stable and direct biotinylated monoclonal antibody of CD_{133} via the streptavidin–biotin interaction. Thus, the cytosensor responded to the lowest number of conjugated cell to the CD_{133} monoclonal antibody. Despite many efforts to identify circulating tumor cells (CTCs), the calculation of CTCs number is not practically applicable due to small fraction of these cells in blood and fluctuation in their population. These conditions do not provide effective information for clinicians to precisely follow up the cancer patients. Perhaps, if more sophisticated cytosensors are developed to detect CSCs, as part of CTCs, and related by products such as exosomes, we will be more successful detection of tumorigenesis in the initial phase and also monitoring of the therapeutic efficiency. Especially, these conditions are vital in patients with

high-degree tumors, because of resistant CSCs. These cells can circulate in body fluids and initiate new tumor foci in remote sites which need to be tracked. To this end, the range of cytosensor detection for certain cell types should be in a way to diagnose minimum CTCs in the initial phase of tumor development. It seems that detection of tumor cells outside this range is not clinically effective because other conventional analytical assays such as CBC, histological examination can help us in the diagnosis of cancer patients. Interestingly, in patients with different cancer types at phases II, III clinical signs are easily detectable.

Supplementary Information

The online version contains supplementary material available at https://doi.org/10.1186/s12645-023-00208-4.

Additional file 1: Figure S1. Dot mapping images of the deposition of MSNs on the GCE, A) Carbon atoms B) Oxygen atoms and C) Oxygen and silica atoms, co-electrodeposition of MSNs/PtNPs nanocomposite, D) Oxygen atoms, E) Platinum atoms, F) Carbon atoms, G) Silica atoms and H) Oxygen, silica and platinum atoms. **Figure S2.** Immobilized stem cells on the modified electrodein different magnifications. **Figure S3.** The selectivity of the biosensor. Comparison of DPV peak heights of somatic cancer cellsand cancer stem cellsat three different concentrations of 5, 15 and 20 cells /mL. **Table S1.** The percentage of carbon, silica, oxygen and platinum atoms in MSN and MSN-PtNPs on the GCE. **Table S2.** Studying of the reproducibility of the cytosensor with two same GC electrodes at concentrations of 20 cells/mL. **Table S3.** Investigation of the stability of the cytosensor via peak heights at concentrations of 15 cells/mL.

Acknowledgements
The authors would like to thank Faculty of Advanced Medical Sciences for funding of this project.

Author contributions
SS contributed to all experimental analysis and preparing of first draft. BK supervised the study and participated in idea, development of the method, validation of data and editing. MM and FSN participated in cell culture and stem cells isolation. II helped in validation of data and editing. SD and MRR contributed to data interpretations. FB was the supervisor of the study and assisted data interpretations. [All authors read and approved the final manuscript.]

Funding
This project was financially supported by faculty of Advanced Medical Sciences, Tabriz University of Medical Sciences, Tabriz, Iran (Grant Number: 67620).

Availability of data and materials
Not applicable.

Declarations

Ethics approval and consent to participate
All patients were asked to complete the informed consent. All procedures of this study were approved by the Local Ethics Committee of Tabriz University of Medical Sciences (IR.TBZMED.VCR.REC.1400.198). All procedures were done under the declaration of Helsinki.

Consent for publication
Not applicable.

Competing interests
The authors declare no competing interest.

Received: 2 April 2023 Accepted: 2 May 2023
Published online: 20 May 2023

References

Babaei A, Zendehdel M, Khalilzadeh B, Abnosi M (2010) A new sensor for simultaneous determination of tyrosine and dopamine using iron (III) doped zeolite modified carbon paste electrode. Chin J Chem 28(10):1967–1972
Baumann M, Krause M, Hill R (2008) Exploring the role of cancer stem cells in radioresistance. Nat Rev Cancer 8(7):545–554
Bomken S, Fišer K, Heidenreich O, Vormoor J (2010) Understanding the cancer stem cell. Br J Cancer 103(4):439–445
Brabletz T, Jung A, Spaderna S, Hlubek F, Kirchner T (2005) Migrating cancer stem cells—an integrated concept of malignant tumour progression. Nat Rev Cancer 5(9):744–749
Bu Y, Cao D (2012) The origin of cancer stem cells. Front Biosci (schol Ed) 4(3):819–830

Chen T, Zhang Y, Guo W, Meng M, Mo X, Lu Y (2010) Effects of heterochromatin in colorectal cancer stem cells on radiosensitivity. Chin J Cancer 29(3):270–276
Chenaghlou S, Khataee A, Jalili R, Rashidi M-R, Khalilzadeh B, Joo SW (2021) Gold nanostar-enhanced electrochemiluminescence immunosensor for highly sensitive detection of cancer stem cells using CD133 membrane biomarker. Bioelectrochemistry 137:107633
Chiou S-H, Wang M-L, Chou Y-T, Chen C-J, Hong C-F, Hsieh W-J, Chang H-T, Chen Y-S, Lin T-W, Hsu H-S (2010) Coexpression of Oct4 and Nanog enhances malignancy in lung adenocarcinoma by inducing cancer stem cell–like properties and epithelial–mesenchymal transdifferentiation. Can Res 70(24):10433–10444
Ciriminna R, Fidalgo A, Pandarus V, Beland F, Ilharco LM, Pagliaro M (2013) The sol–gel route to advanced silica-based materials and recent applications. Chem Rev 113(8):6592–6620
Croker AK, Goodale D, Chu J, Postenka C, Hedley BD, Hess DA, Allan AL (2009) High aldehyde dehydrogenase and expression of cancer stem cell markers selects for breast cancer cells with enhanced malignant and metastatic ability. J Cell Mol Med 13(8b):2236–2252
Dalerba P, Cho RW, Clarke MF (2007a) Cancer stem cells: models and concepts. Annu Rev Med 58:267–284
Dalerba P, Dylla SJ, Park I-K, Liu R, Wang X, Cho RW, Hoey T, Gurney A, Huang EH, Simeone DM (2007b) Phenotypic characterization of human colorectal cancer stem cells. Proc Natl Acad Sci 104(24):10158–10163
de Melo FS, Kurtova AV, Harnoss JM, Kljavin N, Hoeck JD, Hung J, Anderson JE, Storm EE, Modrusan Z, Koeppen H (2017) A distinct role for Lgr5+ stem cells in primary and metastatic colon cancer. Nature 543(7647):676–680
Deepa P, Kanungo M, Claycomb G, Sherwood PM, Collinson MM (2003) Electrochemically deposited sol− gel-derived silicate films as a viable alternative in thin-film design. Anal Chem 75(20):5399–5405
Diehn M, Cho RW, Lobo NA, Kalisky T, Dorie MJ, Kulp AN, Qian D, Lam JS, Ailles LE, Wong M (2009) Association of reactive oxygen species levels and radioresistance in cancer stem cells. Nature 458(7239):780–783
Fachin F, Spuhler P, Martel-Foley JM, Edd JF, Barber TA, Walsh J, Karabacak M, Pai V, Yu M, Smith K (2017) Monolithic chip for high-throughput blood cell depletion to sort rare circulating tumor cells. Sci Rep 7(1):1–11
Farghaly AA, Collinson MM (2014) Electroassisted codeposition of sol–gel derived silica nanocomposite directs the fabrication of coral-like nanostructured porous gold. Langmuir 30(18):5276–5286
Farghaly AA, Collinson MM (2016) Mesoporous hybrid polypyrrole-silica nanocomposite films with a strata-like structure. Langmuir 32(23):5925–5936
Ghoncheh M, Mohammadian M, Mohammadian-Hafshejani A, Salehiniya H (2016) The incidence and mortality of colorectal cancer and its relationship with the human development index in Asia. Ann Glob Health 82(5):726–737
Goux A, Etienne M, Aubert E, Lecomte C, Ghanbaja J, Walcarius A (2009) Oriented mesoporous silica films obtained by electro-assisted self-assembly (EASA). Chem Mater 21(4):731–741
Haggar FA, Boushey RP (2009) Colorectal cancer epidemiology: incidence, mortality, survival, and risk factors. Clin Colon Rectal Surg 22(04):191–197
Hardin H, Zhang R, Helein H, Buehler D, Guo Z, Lloyd RV (2017) The evolving concept of cancer stem-like cells in thyroid cancer and other solid tumors. Lab Invest 97(10):1142–1151
Hasanzadeh M, Karim-Nezhad G, Shadjou N, Khalilzadeh B, Saghatforoush L, Ershad S, Kazeman I (2009) Kinetic study of the electro-catalytic oxidation of hydrazine on cobalt hydroxide modified glassy carbon electrode. Chin J Chem 27(4):638–644
Heddleston J, Li Z, Lathia J, Bao S, Hjelmeland A, Rich J (2010) Hypoxia inducible factors in cancer stem cells. Br J Cancer 102(5):789–795
Hosonuma S, Kobayashi Y, Kojo S, Wada H, Seino K-i, Kiguchi K, Ishizuka B (2011) Clinical significance of side population in ovarian cancer cells. Hum Cell 24(1):9–12
Isildak I, Navaeipour F, Afsharan H, Kanberoglu GS, Agir I, Ozer T, Annabi N, Totu EE, Khalilzadeh B (2020) Electrochemiluminescence methods using CdS quantum dots in aptamer-based thrombin biosensors: a comparative study. Microchim Acta 187:1–13
Karimzadeh Z, Hasanzadeh M, Isildak I, Khalilzadeh B (2020) Multiplex bioassaying of cancer proteins and biomacromolecules: nanotechnological, structural and technical perspectives. Int J Biol Macromol 165:3020–3039
Kazama S, Kishikawa J, Kiyomatsu T, Kawai K, Nozawa H, Ishihara S, Watanabe T (2018) Expression of the stem cell marker CD133 is related to tumor development in colorectal carcinogenesis. Asian J Surg 41(3):274–278
Kolodny G, Li X, Balk S (2018) Addressing cancer chemotherapeutic toxicity, resistance, and heterogeneity: novel theranostic use of DNA-encoded small molecule libraries. BioEssays 40(10):1800057
Kreso A, Dick JE (2014) Evolution of the cancer stem cell model. Cell Stem Cell 14(3):275–291
LaBarge MA (2010) The difficulty of targeting cancer stem cell niches. Clin Cancer Res 16(12):3121–3129
Li Y-f, Xiao B, Tu S-f, Wang Y-y, Zhang X-l (2012) Cultivation and identification of colon cancer stem cell-derived spheres from the Colo205 cell line. Braz J Med Biol Res 45(3):197–204
Liao W-T, Ye Y-P, Deng Y-J, Bian X-W, Ding Y-Q (2014) Metastatic cancer stem cells: from the concept to therapeutics. Am J Stem Cells 3(2):46
Mansouri M, Khalilzadeh B, Barzegari A, Shoeibi S, Isildak S, Bargahi N, Omidi Y, Dastmalchi S, Rashidi M-R (2020) Design a highly specific sequence for electrochemical evaluation of meat adulteration in cooked sausages. Biosens Bioelectron 150:111916
Markowitz SD, Bertagnolli MM (2009) Molecular basis of colorectal cancer. N Engl J Med 361(25):2449–2460
Nasrollahpour H, Khalilzadeh B, Naseri A, Sillanpaa M, Chia CH (2021a) Homogeneous electrochemiluminescence in the sensors game: what have we learned from past experiments? Anal Chem 94(1):349–365
Nasrollahpour H, Isildak I, Rashidi M-R, Hashemi EA, Naseri A, Khalilzadeh B (2021b) Ultrasensitive bioassaying of HER-2 protein for diagnosis of breast cancer using reduced graphene oxide/chitosan as nanobiocompatible platform. Cancer Nanotechnol 12(1):10
Nasrollahpour H, Mahdipour M, Isildak I, Rashidi M-R, Naseri A, Khalilzadeh B (2021c) A highly sensitive electrochemiluminescence cytosensor for detection of SKBR-3 cells as metastatic breast cancer cell line: A constructive phase in early and precise diagnosis. Biosens Bioelectron 178:113023

O'Brien CA, Pollett A, Gallinger S, Dick JE (2007) A human colon cancer cell capable of initiating tumour growth in immunodeficient mice. Nature 445(7123):106–110
Oskarsson T, Batlle E, Massagué J (2014) Metastatic stem cells: sources, niches, and vital pathways. Cell Stem Cell 14(3):306–321
Ozkumur E, Shah AM, Ciciliano JC, Emmink BL, Miyamoto DT, Brachtel E, Yu M, Chen P-i, Morgan B, Trautwein J (2013) Inertial focusing for tumor antigen–dependent and–independent sorting of rare circulating tumor cells. Sci Translat Med 5(179):179147
Pallela R, Chandra P, Noh H-B, Shim Y-B (2016) An amperometric nanobiosensor using a biocompatible conjugate for early detection of metastatic cancer cells in biological fluid. Biosens Bioelectron 85:883–890
Pathania S, Bhatia R, Baldi A, Singh R, Rawal RK (2018) Drug metabolizing enzymes and their inhibitors' role in cancer resistance. Biomed Pharmacother 105:53–65
Rasouliyan F, Eskandani M, Jaymand M, Nakhjavani SA, Farahzadi R, Vandghanooni S, Eskandani M (2021) Preparation, physicochemical characterization, and anti-proliferative properties of Lawsone-loaded solid lipid nanoparticles. Chem Phys Lipid 239:105123
Reya T, Morrison SJ, Clarke MF, Weissman IL (2001) Stem cells, cancer, and cancer stem cells. Nature 414(6859):105–111
Rezapour Sarabi M, Nakhjavani SA, Tasoglu S (2022) 3D-Printed microneedles for point-of-care biosensing applications. Micromachines 13(7):1099
Ricci-Vitiani L, Lombardi DG, Pilozzi E, Biffoni M, Todaro M, Peschle C, De Maria R (2007) Identification and expansion of human colon-cancer-initiating cells. Nature 445(7123):111–115
Ricci-Vitiani L, Fabrizi E, Palio E, De Maria R (2009) Colon cancer stem cells. J Mol Med 87(11):1097
Saghatforoush L, Hasanzadeh M, Karim-Nezhad G, Ershad S, Shadjou N, Khalilzadeh B, Hajjizadeh M (2009) Kinetic study of the electrooxidation of mefenamic acid and indomethacin catalysed on cobalt hydroxide modified glassy carbon electrode. Bull Korean Chem Soc 30(6):1341–1348
Same S, Nakhjavani SA, Samee G, Davaran S (2022) Halloysite clay nanotube in regenerative medicine for tissue and wound healing. Ceram Int. https://doi.org/10.1016/j.ceramint.2022.05.037
Shimokawa M, Ohta Y, Nishikori S, Matano M, Takano A, Fujii M, Date S, Sugimoto S, Kanai T, Sato T (2017) Visualization and targeting of LGR5+ human colon cancer stem cells. Nature 545(7653):187–192
Sibottier E, Sayen S, Gaboriaud F, Walcarius A (2006) Factors affecting the preparation and properties of electrodeposited silica thin films functionalized with amine or thiol groups. Langmuir 22(20):8366–8373
Sun D, Lu J, Zhong Y, Yu Y, Wang Y, Zhang B, Chen Z (2016) Sensitive electrochemical aptamer cytosensor for highly specific detection of cancer cells based on the hybrid nanoelectrocatalysts and enzyme for signal amplification. Biosens Bioelectron 75:301–307
Therese GHA, Kamath PV (2000) Electrochemical synthesis of metal oxides and hydroxides. Chem Mater 12(5):1195–1204
Tian L, Qi J, Qian K, Oderinde O, Cai Y, Yao C, Song W, Wang Y (2018a) An ultrasensitive electrochemical cytosensor based on the magnetic field assisted binanozymes synergistic catalysis of Fe3O4 nanozyme and reduced graphene oxide/molybdenum disulfide nanozyme. Sens Actuators B Chem 260:676–684
Tian L, Qi J, Qian K, Oderinde O, Liu Q, Yao C, Song W, Wang Y (2018b) Copper (II) oxide nanozyme based electrochemical cytosensor for high sensitive detection of circulating tumor cells in breast cancer. J Electroanal Chem 812:1–9
Todaro M, Francipane MG, Medema JP, Stassi G (2010) Colon cancer stem cells: promise of targeted therapy. Gastroenterology 138(6):2151–2162
Tsai LL, Yu CC, Chang YC, Yu CH, Chou MY (2011) Markedly increased Oct4 and Nanog expression correlates with cisplatin resistance in oral squamous cell carcinoma. J Oral Pathol Med 40(8):621–628
Vandghanooni S, Rasoulian F, Eskandani M, Akbari Nakhjavani S, Eskandani M (2021) Acriflavine-loaded solid lipid nanoparticles: preparation, physicochemical characterization, and anti-proliferative properties. Pharm Dev Technol 26(9):934–942
Vinogradov S, Wei X (2012) Cancer stem cells and drug resistance: the potential of nanomedicine. Nanomedicine 7(4):597–615
Wang H, Zhou C, Sun X, Jian Y, Kong Q, Cui K, Ge S, Yu J (2018) Polyhedral-AuPd nanoparticles-based dual-mode cytosensor with turn on enable signal for highly sensitive cell evaluation on lab-on-paper device. Biosens Bioelectron 117:651–658
Wu W, Yu L, Fang Z, Lie P, Zeng L (2013) A lateral flow biosensor for the detection of human pluripotent stem cells. Anal Biochem 436(2):160–164
Wu Z-Y, Chen J-Y, Zhu X, Fu F-H, Lan R-L, Liu M-M, Lian X, Ye C-L, Zhong G-X, Lin J-H (2018) Sensitive electrochemical cytosensor for highly specific detection of osteosarcoma 143B cells based on graphene-3D gold nanocomposites. J Electroanal Chem 824:108–113
Xu J, Hu Y, Wang S, Ma X, Guo J (2020) Nanomaterials in electrochemical cytosensors. Analyst 145(6):2058–2069
Yang M-H, Imrali A, Heeschen C (2015) Circulating cancer stem cells: the importance to select. Chin J Cancer Res 27(5):437
Zhang H, Ke H, Wang Y, Li P, Huang C, Jia N (2019) 3D carbon nanosphere and gold nanoparticle-based voltammetric cytosensor for cell line A549 and for early diagnosis of non-small cell lung cancer cells. Microchim Acta 186(1):1–7
Zheng T, Fu J-J, Hu L, Qiu F, Hu M, Zhu J-J, Hua Z-C, Wang H (2013) Nanoarchitectured electrochemical cytosensors for selective detection of leukemia cells and quantitative evaluation of death receptor expression on cell surfaces. Anal Chem 85(11):5609–5616

Publisher's Note